Effective Theory Analysis of Precision Electroweak Data

Zhenyu Han[*] and Witold Skiba[†]

Department of Physics, Yale University, New Haven, CT 06520

Abstract

We obtain the bounds on arbitrary linear combinations of operators of dimension 6 in the Standard Model. We consider a set of 21 flavor and CP conserving operators. Each of our 21 operators is tightly constrained by the standard set of electroweak measurements. We perform a fit to all relevant precision electroweak data and include neutrino scattering experiments, atomic parity violation, W mass, LEP1, SLD, and LEP2 data. Our results provide an efficient way of obtaining bounds on weakly coupled extensions of the Standard Model.

[*] email address: `zhenyu.han@yale.edu`
[†] email address: `witold.skiba@yale.edu`

I. INTRODUCTION

Despite the enormous success of the Standard Model (SM), we are certain that the SM is an effective theory with a cutoff that is much smaller than the Planck scale. A lot of effort is being devoted to constructing and studying extensions of the SM that predict new particles having TeV scale masses. An integral part of this effort is constraining the parameters of new models using experimental data. In many cases, the constraints are obtained by directly computing the deviations from the SM that are induced by new particles in a specific model.

An effective field theory approach is a two step process. First, one integrates out all new heavy states and obtains effective interactions involving only fields of the SM. These new effective higher-dimensional operators are then used to compute the deviations from the SM and compare with the experimental data. Following this approach one needs to make contact with experimental data only once—by computing the effects of higher-dimensional operators on different experiments and obtaining bounds on the coefficients of such operators using the data. Once this step is completed, one can constrain any model just by calculating the coefficients of new effective operators.

The effective theory approach is by no means new, and has been applied to the electroweak data many times. Lucid explanation on applying effective Lagrangians to precision electroweak measurements can be found, for example, in Refs. [1, 2]. Perhaps the best known example of the effective approach are the so-called oblique corrections [3, 4]. The oblique corrections only modify the SM gauge boson propagators. The formalism of oblique corrections has been extended in Refs. [5, 6]. While in many models new physics contributions are limited to two point functions of gauge bosons, it is not always the case.

In this article we study bounds on the coefficients of effective operators that could be relevant for the physics of electroweak symmetry breaking. We assume that just above the electroweak scale the $SU(2)_L \times U(1)_Y$ gauge symmetry is linearly realized and therefore the field content involves a scalar electroweak doublet. This determines the power counting and our effective Lagrangian

$$\mathcal{L} = \mathcal{L}_{SM} + a_i \, O_i \tag{1}$$

contains operators of dimension 6 in addition to the SM Lagrangian. Therefore each coefficient a_i has the dimension of inverse mass squared and can be conveniently represented as $a_i = \frac{1}{\Lambda_i^2}$. In our analysis, we include 21 operators—two of which correspond to the S and T parameters [4]. Our choice of operators O_i is explained in the next section. In summary, we choose operators that conserve $U(3)^5$ flavor symmetry of the SM, as well as conserve CP. We also restrict ourselves to operators that are stringently constrained by the usual set of electroweak precision measurements. There is a number of dimension 6 operators that are flavor and CP conserving but the available data is not accurate enough to place stringent bounds on the corresponding Λ_i's. The bounds on the scales Λ_i of the 21 individual operators in our basis are all about 1 TeV or higher. In contrast, the bounds on flavor conserving four-quark contact interactions or operators involving quarks and gluons are usually much lower. While it is exciting that operators suppressed by relatively low scales Λ are allowed, such operators are not very useful for constraining new models.

Because of the spectacular agreement between the SM and precision experiments the allowed deviations from the SM are small. Therefore, when computing the effects of operators O_i in Eq. (1) we can restrict ourselves to computing only the interference terms between $\mathcal{L}_{SM}$ and the operators O_i. In other words, we work to the linear order in the coefficients a_i. Expansion in powers of a_i corresponds to expansion in $\frac{E^2}{\Lambda_i^2}$ or $\frac{v^2}{\Lambda_i^2}$, where E is the charac-

teristic energy scale of a given process and v is the Higgs vacuum expectation value (vev). Given that $E, v \ll \Lambda_i$, neglecting the terms quadratic in a_i is a good approximation. The SM predictions can be computed to arbitrary accuracy since they do not depend on a_i. We then compare the results with the experimental data and compute the χ^2 distribution as a function of a_i. Since our results are linear in the coefficients a_i, χ^2 is quadratic in a_i and can be written as

$$\chi^2(a_i) = \chi^2_{min} + (a_i - \hat{a}_i)\mathcal{M}_{ij}(a_j - \hat{a}_j), \tag{2}$$

where $\hat{a}_i$ are the values of a_i that minimize χ^2.

The main result of our paper is the matrix $\mathcal{M}_{ij}$ and the vector $\hat{a}_i$ in Eq. (2). We would like to stress an obvious point here—the coefficients $\mathcal{M}_{ij}$ and $\hat{a}_i$ are constants that we obtain by fitting to experimental data. Given this, admittedly, large set of numbers one can compute the bounds on any linear combination of operators O_i in our basis. Integrating out heavy particles from an extension of the SM will, in general, lead to a set of operators O_i whose coefficients are correlated by the underlying theory. Since we are working in the linear approximation in terms of the coefficients a_i, the effects of correlated operators are also linear and the analysis of bounds on a new model remains very simple. Readers interested in applying our work to their favorite model can use Eq. (2) and skip all the details on how we obtain the χ^2 distribution.

An effective Lagrangian analysis has been performed in many cases in the past. For examples see Refs. [1, 2, 7, 8, 9, 10, 11]. Ref. [10] is perhaps the closest to our approach, but it only includes the operators constrained by the Z-pole measurements and considers bounds on individual operators. We focus on a broader set of effective operators and use the results from LEP1, SLD, LEP2, as well as lower energy experiments to bound the coefficients of the effective operators. The most important set of precision electroweak measurements come from LEP and SLD. Since these experiments no longer collect data, the precision of the data relevant for our analysis is not going to significantly improve in the near future.

In the next section we enumerate the operators in our basis. We further explain what motivates our choice of the 21 operators. In Sec. III, we list the experiments that we use to obtain the bounds on the effective operators. We outline our calculations of the interference terms between the SM and the additional operators in Sec. IV, and describe the numerical analysis in Sec. V. We summarize the results in Sec. VI. Our numerical results are presented in Appendix A. We show how to use these results in Appendix B by reproducing the bounds on the S and T parameters. Another example is provided in Appendix C, where we illustrate our procedure on Z' gauge bosons and compare our results with Ref. [12]. We performed the numerical analysis using Mathematica, and we make the notebooks available online. A few comments about our code are contained in Appendix D.

II. OPERATORS

We assume that just above the electroweak symmetry breaking scale, the effective theory is that of the SM with one Higgs doublet. In our effective theory the $SU(2)_L \times U(1)_Y$ symmetry is linearly realized. The assumption of one Higgs doublet is not at all relevant since it is only the vev of the Higgs that enters the analysis. Since the electroweak symmetry is linearly realized the physical Higgs and the electroweak breaking vev are assigned mass dimension one. The vev appearing in the Lagrangian is always raised to positive powers. In case of nonlinearly realized electroweak symmetry, the expansion parameter is the momen-

tum divided by the vev times 4π. A number of authors studied electroweak precision data in nonlinear realizations of electroweak symmetry, for examples see Refs. [8, 13, 14].

A complete set of dimension-6 operators consistent with the $SU(3) \times SU(2)_L \times U(1)_Y$, baryon and lepton number conservation and the linearly realized electroweak symmetry has been presented in Ref. [1]. There are 80 operators in the basis of Ref. [1] after the leading order equations of motion are used to obtain an independent set of operators [15, 16].

We are interested in constraining models of new physics pertinent to the electroweak symmetry breaking. Processes that contribute to flavor or CP violation have to be suppressed by scales much higher than the electroweak scale. A typical suppression for four fermion operators that contribute to the $K - \bar{K}$ mass difference is about 10^3 TeV [1]. The bounds are even more stringent in the lepton sector: about 10^4 TeV suppression is required for the electric dipole moment of the electron [17, 18]; the limits on the $\mu \to e\gamma$ decay also imply 10^4 TeV suppression for the contributing operators [1]. Thus it is natural to assume that the electroweak scale and the scales associated with flavor and CP violation are well separated. Processes involving the third generation are an obvious exception. Experiments have limited statistics and new flavor-dependent physics at TeV scale is possible. It is plausible that the third generation actively participates in the electroweak symmetry breaking. This interesting case merits a separate study but is beyond the scope of this article. We therefore impose $U(3)^5$ flavor symmetry on our operators. A different $U(3)$ acts on the left-handed quarks and leptons as well as on the right handed quarks and leptons. Consequently, our operators are unchanged when written in terms of either mass or gauge eigenstates.

Among the 80 operators of dimension 6 listed in Ref. [1], there are 28 operators that do not conserve CP or flavor $U(3)^5$, or violate both. Among the remaining 52 operators there are 18 operators that only involve quark and/or gluon fields. The bounds on such operators are poor since the precision of hadron experiments is not comparable to that of the e^+e^- machines. Such operators are therefore not helpful in constraining models with new physics at the TeV scale.

Thus, there are 34 operators that conserve flavor and CP and contain either electroweak gauge bosons or leptons and perhaps some quark fields. Six of these 34 operators are not observable in current experiments: either they contribute to dimension 4 couplings in the SM Lagrangian or they involve the Higgs doublet only.

We are finally left with 28 operators. Seven operators in this set are of the form

$$O_{fF} = i(\bar{f}\gamma^\mu D^\nu f) F_{\mu\nu}, \tag{3}$$

where f represents a fermion and $F_{\mu\nu}$ is the field strength for the hypercharge or weak gauge bosons. These operators can only contribute to the Z-pole measurements. At other energies the interference term between the SM contribution and the contribution of operators O_{fF} vanishes since one of the contributions is real and the other is imaginary. For the same reason the interference term at the Z pole is suppressed by the ratio of the Z width to the Z mass. We therefore neglect the operators O_{fF} in our analysis.

We choose the following basis for the remaining 21 operators that are the focus of our work. Our notation is standard: q and l represent the three families of the left-handed quark and lepton fields, respectively. The right handed fields are labeled u, d, and e. We omit the family index which is always summed over due to the flavor $U(3)^5$ symmetry. We adopt the notation of Ref. [1] with minor modifications and in a few cases our operators do differ from Ref. [1] by a numerical factor.

4

The operators that contain only the gauge bosons and Higgs doublets are

$$O_{WB} = (h^\dagger \sigma^a h) W^a_{\mu\nu} B^{\mu\nu}, \quad O_h = |h^\dagger D_\mu h|^2, \tag{4}$$

where $W^a_{\mu\nu}$ is the $SU(2)$ field strength, $B_{\mu\nu}$ the hypercharge field strength, and h represents the Higgs doublet. There are 11 four-fermion operators. These are

$$O^s_{ll} = \frac{1}{2}(\bar{l}\gamma^\mu l)(\bar{l}\gamma_\mu l), \quad O^t_{ll} = \frac{1}{2}(\bar{l}\gamma^\mu \sigma^a l)(\bar{l}\gamma_\mu \sigma^a l), \tag{5}$$

$$O^s_{lq} = (\bar{l}\gamma^\mu l)(\bar{q}\gamma_\mu q), \quad O^t_{lq} = (\bar{l}\gamma^\mu \sigma^a l)(\bar{q}\gamma_\mu \sigma^a q), \tag{6}$$

$$O_{le} = (\bar{l}\gamma^\mu l)(\bar{e}\gamma_\mu e), \quad O_{qe} = (\bar{q}\gamma^\mu q)(\bar{e}\gamma_\mu e), \tag{7}$$

$$O_{lu} = (\bar{l}\gamma^\mu l)(\bar{u}\gamma_\mu u), \quad O_{ld} = (\bar{l}\gamma^\mu l)(\bar{d}\gamma_\mu d), \tag{8}$$

$$O_{ee} = \frac{1}{2}(\bar{e}\gamma^\mu e)(\bar{e}\gamma_\mu e), \quad O_{eu} = (\bar{e}\gamma^\mu e)(\bar{u}\gamma_\mu u), \quad O_{ed} = (\bar{e}\gamma^\mu e)(\bar{d}\gamma_\mu d). \tag{9}$$

The operators in Eqs. (5) and (6) involve only left-handed fields, in Eqs. (7) and (8) 2 left-handed and 2 right-handed, while in Eq. (9) all right-handed fields. There are 7 operators containing 2 fermions that alter the couplings of fermions to the gauge bosons

$$O^s_{hl} = i(h^\dagger D^\mu h)(\bar{l}\gamma_\mu l) + \text{h.c.}, \quad O^t_{hl} = i(h^\dagger \sigma^a D^\mu h)(\bar{l}\gamma_\mu \sigma^a l) + \text{h.c.}, \tag{10}$$

$$O^s_{hq} = i(h^\dagger D^\mu h)(\bar{q}\gamma_\mu q) + \text{h.c.}, \quad O^t_{hq} = i(h^\dagger \sigma^a D^\mu h)(\bar{q}\gamma_\mu \sigma^a q) + \text{h.c.}, \tag{11}$$

$$O_{hu} = i(h^\dagger D^\mu h)(\bar{u}\gamma_\mu u) + \text{h.c.}, \quad O_{hd} = i(h^\dagger D^\mu h)(\bar{d}\gamma_\mu d) + \text{h.c.}, \tag{12}$$

$$O_{he} = i(h^\dagger D^\mu h)(\bar{e}\gamma_\mu e) + \text{h.c.} . \tag{13}$$

Finally, there is an operator that modifies the triple gauge boson interactions

$$O_W = \epsilon^{abc} W^{a\nu}_\mu W^{b\lambda}_\nu W^{c\mu}_\lambda. \tag{14}$$

Eqs. (4) through (14) define our basis of the 21 operators.

We denote the coefficients a_i in the Lagrangian in Eq. (1) using the same indices as the corresponding operators, so that the effective Lagrangian is

$$\mathcal{L} = \mathcal{L}_{SM} + a_{WB} \, O_{WB} + a_h \, O_h + \ldots + a_W \, O_W. \tag{15}$$

Note that the first two operators in our basis, O_{WB} and O_h, are in a one-to-one relation with the S and T parameters [4]. The correspondence is

$$a_{WB} = \frac{1}{4sc}\frac{\alpha}{v^2}S, \; a_h = -2\frac{\alpha}{v^2}T, \tag{16}$$

where $\langle h \rangle = \begin{pmatrix} 0 \\ v/\sqrt{2} \end{pmatrix}$, α is the fine-structure constant, s and c are the sine and cosine of the weak mixing angle, respectively. The U parameter is related to a dimension-8 operator in our power counting scheme and therefore does not appear in our analysis.

III.   EXPERIMENTS

The three most precisely measured electroweak sector observables: α, G_F, and M_Z are taken to be the input parameters, from which the SM gauge couplings and the Higgs vev are

	Standard Notation	Measurement	Reference
Atomic parity	$Q_W(Cs)$	Weak charge in Cs	[21]
violation	$Q_W(Tl)$	Weak charge in Tl	[22]
DIS	g_L^2, g_R^2	ν_μ-nucleon scattering from NuTeV	[23]
	R^ν	ν_μ-nucleon scattering from CDHS and CHARM	[24, 25]
	κ	ν_μ-nucleon scattering from CCFR	[26]
	$g_V^{\nu e}, g_A^{\nu e}$	ν-e scattering from CHARM II	[27]
Z-pole	Γ_Z	Total Z width	[20]
	σ_h^0	e^+e^- hadronic cross section at Z pole	[20]
	$R_f^0 (f = e, \mu, \tau, b, c)$	Ratios of decay rates	[20]
	$A_{FB}^{0,f}(f = e, \mu, \tau, b, c)$	Forward-backward asymmetries	[20]
	$\sin^2\theta_{eff}^{lept}(Q_{FB})$	Hadronic charge asymmetry	[20]
	$A_f(f = e, \mu, \tau, b, c)$	Polarized asymmetries	[20]
Fermion pair	$\sigma_f(f = q, \mu, \tau)$	Total cross sections for $e^+e^- \to f\overline{f}$	[20]
production at	$A_{FB}^f(f = \mu, \tau)$	Forward-backward asymmetries for $e^+e^- \to f\overline{f}$	[20]
LEP2	$d\sigma_e/d\cos\theta$	Differential cross section for $e^+e^- \to e^+e^-$	[28]
W pair	$d\sigma_W/d\cos\theta$	Differential cross section for $e^+e^- \to W^+W^-$	[29]
	M_W	W mass	[20, 30]

TABLE I: Relevant measurements

inferred. Predictions for experiments are computed in terms of the inputs and the coefficients of the new operators. The experimental quantities we use to constrain the coefficients of operators are listed in Table I. Detailed descriptions and references for individual experiments can be found in many reviews, for example in Refs. [19] and [20].

The list of experiments in Table I does not include the anomalous magnetic moment of the muon [31], one of the most precisely measured electroweak quantities. The operators that contribute directly to $(g-2)$ involve left and right-handed fields and are not $U(3)^5$ invariant. There are also loop contributions from operators like O_{WB}, O_W, and many four-fermion operators. Such loop contributions are divergent and require introducing counterterms in the form of operators excluded from our analysis due to their lack of $U(3)^5$ invariance. An operator analysis of contributions to the muon $(g-2)$ can be found in Ref. [32].

For a given observable X, our prediction can be written as:

$$X_{th} = X_{SM} + \sum_i a_i X_i, \tag{17}$$

where X_{th} is the prediction in the presence of additional operators, X_{SM} is the standard model prediction and $\sum_i a_i X_i$ are corrections from our new operators. In practice, the SM predictions are computed to the required accuracy in perturbation theory and are well known for all the measurements we use. Note that the corrections X_i arise in two different ways. First, an operator can generate a new Feynman diagram contributing to a given physical process. For example, a four-fermion operator O_{le} enters the $e^+e^- \to \mu^+\mu^-$ process as a new diagram, in addition to the Z and γ exchange diagrams. We call this "direct" correction. Second, some operators can shift the input parameters, because they add new diagrams to the physical processes based on which α, G_F, and M_Z are measured. Thus, the input parameters determined from these observables are different from their SM values. Since

all the other observables are calculated from these input parameters, they will inevitably receive indirect corrections from the shifts. We summarize the direct and indirect effects of our operators in Table II.

Because of their high statistics, the Z-pole data and several best measured low-energy observables dominate the bounds on the coefficients a_i whenever such measurements constrain an operator. This is the case for the operators that shift the input parameters and the operators of the form O_{hf}, which change the couplings between the Z boson and the fermions. The four-fermion operators do not contribute to the Z-pole measurements at the linear order, that is the interference term between the SM contribution and the four-fermion operators vanishes at the Z pole. Therefore, to constrain four-fermion operators we have to include the cross sections for fermion-pair production at LEP2. We also include the differential cross sections for the W pair production to constrain the operator O_W. There are several operators, in addition to O_W, that alter the cross section for W pair production. However, these operators are well bounded by other measurements and the W pair production does not contribute significantly to the bounds on their coefficients.

Operator(s)	shift	M_W	Z-pole	DIS	Q_W	$e^+e^- \to f\overline{f}$ (LEP2)	$e^+e^- \to W^+W^-$
O_{WB}	α, M_Z		$\checkmark$	$\checkmark$	$\checkmark$	$\checkmark$	$\checkmark$
O_h	M_Z						
O_{ll}^t	G_F			$\checkmark$		$\checkmark$	
O_{ll}^s, O_{le}				$\checkmark$		$\checkmark$	
O_{ee}						$\checkmark$	
$O_{lq}^s, O_{lq}^t, O_{lu}, O_{ld}$				$\checkmark$	$\checkmark$	$\checkmark$	
O_{eq}, O_{eu}, O_{ed}					$\checkmark$	$\checkmark$	
O_{hl}^t	G_F		$\checkmark$	$\checkmark$	$\checkmark$	$\checkmark$	$\checkmark$
O_{hl}^s, O_{he}			$\checkmark$	$\checkmark$	$\checkmark$	$\checkmark$	$\checkmark$
$O_{hu}, O_{hd}, O_{hq}^s, O_{hq}^t$			$\checkmark$	$\checkmark$	$\checkmark$	$\checkmark$	
O_W							$\checkmark$

TABLE II: Measurements influenced by different operators. The check marks, $\checkmark$, indicate "direct" corrections only. When an operator contributes to one of the input parameters, the corresponding shift of the input parameter does affect all measurements.

IV.   CALCULATIONS

In this section we describe the computation of the effects of dimension-6 operators. Since a lot of work on this topic is already available in the literature, we quote the results whenever available. We have independently verified all the quoted results.

We work in the linear approximation in terms of the coefficients a_i. As we indicated in the previous section, there are two ways that terms linear in a_i arise. First, as a result of additional Feynman diagrams due to the dimension-6 operators. In this case we simply compute the interference terms between the new operators and the tree-level contribution in the SM. Second, a few of our operators redefine the input parameters inferred from the measurements of α, M_Z, and G_F. We use the tree-level SM results and expand to the linear

order in the deviations induced by the coefficients a_i. One of the most transparent ways of dealing with the shifts of the input parameters is described in Ref. [9].

To track down all the shifts, we find it convenient to use the following parameters in the SM Lagrangian: e, s, and M_Z; or equivalently g, g', and M_Z. They are related to the input parameters and the new operators as

$$e^2 = e_0^2(1 - 2v^2 sc\, a_{WB}), \tag{18}$$

$$M_Z^2 = M_{Z0}^2(1 + 2v^2 sc\, a_{WB} + \frac{v^2}{2}a_h), \tag{19}$$

$$\frac{1}{v^2} = \frac{1}{v_0^2} + 2a_{hl}^t - a_{ll}^t, \tag{20}$$

where

$$\alpha = \frac{e_0^2}{4\pi}, \quad G_F = \frac{1}{\sqrt{2}v_0^2} = \frac{e_0^2}{4\sqrt{2}s_0^2 c_0^2 M_{Z0}^2}. \tag{21}$$

Parameters with subscripts 0 are the values derived in the absence of any additional operators. Eqs. (18) and (19) are the shifts due to the S and T parameters.

The corrections induced by S and T are given in Ref. [4], and can be easily translated to our notation using Eq. (16). Ref. [4] does not provide formulas for LEP2, but the extension to LEP2 is simple. The operator O_{WB} also contains a triple gauge boson coupling, which contributes to the $e^+e^- \to W^+W^-$ process. We discuss this at the end of this section.

The operators with 2 Higgs doublets and 2 fermions, O_{hf}, alter the couplings between gauge bosons and fermions. The changes to the Z-fermion couplings, g_V^f and g_A^f, are given in Ref. [10]. (The v^2 in Ref. [10] is defined as one half of our value.) These changes affect all measurements involving a Z-exchange diagram. We have calculated the SM tree-level predictions in terms of arbitrary g_V^f and g_A^f, so it is easy to obtain the corrections induced by O_{hf}. In addition, the operators O_{hl}^t and O_{hq}^t change the couplings of the W boson to the leptons and quarks:

$$g \to g(1 + v^2 a_{hl}^t) \qquad (W - \text{leptons coupling}), \tag{22}$$

$$g \to g(1 + v^2 a_{hq}^t) \qquad (W - \text{quarks coupling}). \tag{23}$$

These changes enter, besides the shift to G_F, the calculations of the $e^+e^- \to W^+W^-$ cross section in the ν exchange channel, and the ν-nucleon scattering charged current cross sections.

The operator O_{ll}^t shifts the value of the input parameter inferred from G_F. All other four-fermion operators do not contribute to the Z-pole measurements. However, they contribute to the low-energy measurements and LEP2 measurements. We now enumerate the effects of four-fermion operators on the relevant observables:

1. The weak charges measured in atomic parity violation experiments

$$Q_W(Z, N) = -2[(2Z + N)C_{1u} + (Z + 2N)C_{1d}]. \tag{24}$$

C_{1u} and C_{1d} receive corrections

$$\Delta C_{1u} = \frac{\sqrt{2}}{4G_F}(-a_{lq}^s + a_{lq}^t + a_{eu} + a_{qe} - a_{lu}), \tag{25}$$

$$\Delta C_{1d} = \frac{\sqrt{2}}{4G_F}(-a_{lq}^s - a_{lq}^t + a_{ed} + a_{qe} - a_{ld}). \tag{26}$$

8

2. ν-nucleon scattering. The 4-fermion operators affect both the neutral current and the charged current cross sections. The corrections to the couplings $g_L^u, g_L^d, g_R^u, g_R^d$ are

$$\Delta g_{L,eff}^u = \frac{1}{2\sqrt{2}G_F}[-a_{lq}^s + (2g_L^u - 1)a_{lq}^t], \tag{27}$$

$$\Delta g_{L,eff}^d = \frac{1}{2\sqrt{2}G_F}[-a_{lq}^s + (2g_L^d + 1)a_{lq}^t], \tag{28}$$

$$\Delta g_{R,eff}^u = \frac{1}{2\sqrt{2}G_F}(-a_{lu}^s + 2g_R^u a_{lq}^t), \tag{29}$$

$$\Delta g_{R,eff}^d = \frac{1}{2\sqrt{2}G_F}(-a_{ld}^s + 2g_R^d a_{lq}^t). \tag{30}$$

These corrections are "effective" in the sense that they are not corrections to the Z-fermion couplings and thus the formulas above only apply to the ν-nucleon scattering. The corrections to the measured quantities can be easily calculated from the above equations, for example, $g_L^2 = (g_L^u)^2 + (g_L^d)^2$ measured at NuTeV receive the correction

$$\Delta(g_L^2) = 2g_L^u \Delta g_{L,eff}^u + 2g_L^d \Delta g_{L,eff}^d. \tag{31}$$

3. ν-e scattering. The corrections to the coupling $g_V^{\nu e}$ and $g_A^{\nu e}$ are

$$\Delta g_{V,eff}^{\nu e} = \frac{1}{2\sqrt{2}G_F}(-a_{ll}^s + a_{ll}^t - a_{le}), \tag{32}$$

$$\Delta g_{A^e ff}^{\nu e} = \frac{1}{2\sqrt{2}G_F}(-a_{ll}^s + a_{ll}^t + a_{le}). \tag{33}$$

Again, these corrections are "effective" that is only apply to the ν-e scattering process.

4. Fermion pair production at LEP2 energies. The differential cross sections in the presence of the contact operators are given, for example, in Ref. [33].

Finally, the operators O_W and O_{WB} alter the triple gauge boson couplings. After substituting the vev for the Higgs doublet, the two operators yield the following couplings

$$\Delta \mathcal{L} = ia_{WB}v^2 g W_\mu^+ W_\nu^- (cA^{\mu\nu} - sZ^{\mu\nu}) + 6ia_W W_\nu^{-\mu} W_\mu^{+\lambda}(sA_\lambda^\nu + cZ_\lambda^\nu). \tag{34}$$

The tree-level $e^+e^- \to W^+W^-$ differential cross section is calculated in Ref. [34] for arbitrary triple gauge boson couplings. Our effective couplings, Eq. (34), correspond to the terms multiplying κ_V and λ_V in Eq. (2.1) in Ref. [34]. To obtain the cross section we substitute

$$\Delta \kappa_\gamma = \frac{v^2 c}{s} a_{WB}, \tag{35}$$

$$\Delta \kappa_Z = -\frac{v^2 s}{c} a_{WB}, \tag{36}$$

$$\Delta \lambda_\gamma = \Delta \lambda_Z = \frac{3v^2 g}{2} a_W. \tag{37}$$

where Δ's denote the deviations from the SM values.

9

V. TOTAL χ^2 DISTRIBUTION

In the previous section, we described how to compute the changes of observable quantities induced by the operators. Given theses results we calculate the total χ^2 distribution. For non-correlated measurements,

$$\chi^2(a_i) = \sum_X \frac{(X_{th}(a_i) - X_{exp})^2}{\sigma_X^2}, \qquad (38)$$

where X_{exp} is the experimental value for observable X and σ_X is the total error both experimental and theoretical. The experimental values for the observables are obtained from the references cited in Table I. The input parameters and the SM predictions, except those for LEP2, are obtained from Ref. [19], where the following input parameters are used:

$$m_{Higgs} = 113 \text{ GeV}, \ m_{top} = 176.9 \text{ GeV}, \ \alpha_s(M_Z) = 0.1213 \qquad (39)$$

in addition to M_Z, α, and G_F. The uncertainty in the values of the input parameters are incorporated as theory errors on the SM predictions and combined later with experimental errors. For the DIS measurements of CDHS, CHARM and CCFR, we use the SM predictions in Ref. [35], but have corrected them for the small differences of input parameters [36]. The sensitivities of the SM predictions for the $e^+e^- \rightarrow f^+f^-(f \neq e)$ cross sections at LEP2 and the $e^+e^- \rightarrow W^+W^-$ cross section to small changes of the input parameters are negligible compared to experimental errors, as we have verified using ZFITTER [37] and RacoonWW [38]. Therefore, we use the SM predictions provided in the corresponding experimental references. The SM prediction for the $e^+e^- \rightarrow e^+e^-$ (LEP2) differential cross section is calculated using the program BHWIDE [39], assuming the same input parameters as in Eq. (39).

The SM predictions agree with the experimental values well, except for a significant discrepancy for g_L^2 obtained by the NuTeV collaboration [23]. We include the NuTeV result in our calculation, but one could easily omit this result from the χ^2 calculation. We also note that the LEP2 results for the $e^+e^- \rightarrow q\bar{q}$ total cross sections are larger than the SM predictions fairly consistently across different energies probed by LEP2. If we tried to constrain the coefficients of four-fermion operators with two leptons and two quarks using only the $e^+e^- \rightarrow q\bar{q}$ total cross sections, we would get relatively weak bounds on the coefficients a_i of such operators. Weak bounds mean that the the contributions quadratic in the corrections in a_i's should not be neglected, contrary to what we do. However, this discrepancy is not supported by other data that also constrains the same operators. A combined fit to all observables does not yield any coefficients a_i large enough to invalidate the linear approximation. Therefore we suspect this pattern is caused by a systematic error.

Higher order terms in perturbation theory alter our tree-level calculation of the interference terms between the SM and the additional operators. The most important effect in electron-positron scattering is the initial state QED radiation. In order to assess the effect of the radiative corrections, we compare the bounds on the 4-fermion contact operators for the $e^+e^- \rightarrow l^+l^-(l \neq e)$ and $e^+e^- \rightarrow q\bar{q}$ channels with the results given in Ref. [20], Table 8.13. In Ref. [20], the $e^+e^- \rightarrow q\bar{q}$ channel is constrained using the inclusive hadronic total cross sections. The $e^+e^- \rightarrow l^+l^-(l \neq e)$ channel is constrained using the total cross sections and asymmetries for $l = \mu, \tau$ and assuming equal coefficients for the contact terms with μ and τ. For the purpose of comparison we use the same data sets and carry out the same

10

fits. In our final results, of course, all the data is taken into account to obtain the bounds on contact operators.

The comparison was carried out for different contact interactions. (The coefficients of 4-fermion operators in Ref. [20] differ from our coefficients a_i by a factor of 4π.) Several radiative corrections and second order terms in a_i are considered when obtaining bounds on these coefficients[1]. We have obtained bounds for the coefficients of operators neglecting radiative corrections but including second order terms in a_i. Except for one case, the differences between our bounds and the bounds in Ref. [20] for errors on a_i are less than 20%, and for centra values of a_i are less than 0.2σ. When translated to the scale Λ, the difference is less than 10%, which is satisfactory for our purposes. The exception is the bound for the "LR" interaction for $e^+e^- \to q\overline{q}$ channel, which corresponds to a_{lu} and a_{ld} in our notation, in which case the errors quoted in Ref. [20] are much more asymmetric than our estimate of errors. However, the central value of the coefficients differs less than 0.2σ. Since the contact terms with two leptons and two quarks can be constrained much more stringently by the low energy measurements, this discrepancy cannot significantly affect our global fit.

For $e^+e^- \to f^+f^-$ ($f \neq e$) channels, we have also implemented the initial-state photonic correction to the order $O(\alpha)$, which includes initial state soft photon exponentiation and hard photon emission [37]. This correction is the largest radiative correction and we have obtained better agreement with Ref. [20] by including it. Except for the "LR" interaction in the $e^+e^- \to q\overline{q}$ channel mentioned previously, the discrepancies between our errors and central values of a_i and the results of [20] are within 10% and 0.1σ respectively. The remaining discrepancy likely arises from the final state radiative correction, pair production correction and higher order corrections, that we have not implemented.

We can safely neglect effects that contribute at a 10% level to our estimates of the coefficients a_i, we have nevertheless included the first order initial state QED corrections to $e^+e^- \to f^+f^-$ ($f \neq e$) channels in our calculation of χ^2. A factor of $(1 + \alpha_s/\pi)$ is also used to account for the QCD corrections for the hadronic final states [41].

Eq. (38) must be modified to account for the correlations between different measurements. There are three categories of data for which the correlations between measurements cannot be neglected. These are the correlations between Z-pole observables [20], the experimental error correlations for the hadronic total cross sections at LEP2 energies [20]; and the theoretical and experimental error correlations for $e^+e^- \to e^+e^-$ differential cross sections [42]. Including correlations,

$$\chi^2(a_i) = \sum_{p,q}(X_{th}^p(a_i) - X_{exp}^p)(\sigma^2)_{pq}^{-1}(X_{th}^q(a_i) - X_{exp}^q), \tag{40}$$

where the error matrix σ^2 is related to the standard deviations σ_p and the correlation matrix ρ_{pq} as folows

$$\sigma_{pq}^2 = \sigma_p\rho_{pq}\sigma_q. \tag{41}$$

Note that often the correlations for the theoretical, statistical and systematic errors are different, and one should take this into account when computing the final error matrix.

Numerical results for the χ^2 distribution are presented in Appendix A.

---

[1] The radiative corrections are not mentioned in Ref. [20], but are described in results of individual experiments at LEP2. See, for example, Refs. [28] [40].

VI. SUMMARY

We have obtained bounds on the coefficients of 21 dimension 6 operators in the SM. Our analysis is linear in the coefficients of these operators. Therefore, the deviations from the SM predictions arise as interference terms between the SM and the dimension 6 operators. As is often the case, integrating out heavy particles leads not to just one but to several operators whose coefficients are related in terms of the masses and coupling constants of the heavy states. A global analysis of precision electroweak measurements must take into account all new operators induced by integrating out heavy states and account for relations between the coefficients of such operators. Our analysis allows obtaining bounds not just on each individual operator, but on their linear combinations as well. Doing so, in the linear approximation, does not require complicated numerical analysis, and can be done efficiently using our results. Of course, if the new physics contributions are "oblique" or "universal" only, [4, 6], one does not need the whole set of 21 operators. A subset of our operators that only modify SM gauge boson propagators has already been considered in Refs. [4, 6]

Our analysis is accomplished by computing the χ^2 distribution as a function of the coefficients a_i. In the linear approximation, χ^2 takes the form shown in Eqs. (2) and (A1). We concentrated on flavor and CP conserving operators. Such operators are allowed in the SM when suppressed by scales of the order of a few TeV. Generic flavor and CP violating operators must be suppressed by much higher scales. This wide separation of characteristic scales suggests that the electroweak symmetry breaking and the flavor and CP violating sectors can be analyzed independently of one another. We excluded from our analysis operators that are not tightly constrained by the data, for example operators involving only quarks and gluons. Such operators are not helpful in constraining extensions of the SM.

The bounds on the coefficients of individual operators, by which we mean that the SM Lagrangian is amended by only one operator at a time, can be easily obtained from Eq. (2). The $1\,\sigma$ bound on a coefficient a_k is $\hat{a}_k \pm \sqrt{\mathcal{M}_{kk}^{-1}}$, where $\mathcal{M}_{kk}$ indicates a diagonal element of $\mathcal{M}$ and is not summed over k. The fourth roots of the diagonal elements, $\sqrt[4]{\mathcal{M}_{kk}}$, vary from 1.3 TeV to 17 TeV, which is a measure of how rapidly χ^2 changes as a function of $a_k = \frac{1}{\Lambda_k^2}$.

What is interesting is that the eigenvalues of $\mathcal{M}$ vary over a much wider range, their fourth roots span from 180 GeV to 21 TeV. In particular, the fourth roots of the four smallest eigenvalues are 180, 250, 390 and 420 GeV. This means that four linear combinations of the operators are much more weakly constrained than the individual operators. The emergence of these "weakly bounded directions" in the operator space is an interesting byproduct of our analysis. Of course, one can not trust the exact bounds on the "weakly bounded" operators. The linear analysis is not applicable when the suppression scales are so low. One needs to work to the quadratic order in the coefficients to reliably determine the bounds. However, it is clear that the bounds on such linear combinations of operators are quite weak and below 1 TeV. It is interesting to find out if there are heavy particles that yield one of the weakly constrained combination of operators when integrated out. This possibility is currently being investigated.

APPENDIX A: THE MATRIX

Our main result can be presented in two alternative ways

$$\chi^2 = \chi^2_{min} + (a_i - \hat{a}_i)\mathcal{M}_{ij}(a_j - \hat{a}_j) = \chi^2_{SM} + a_i\hat{v}_i + a_i\mathcal{M}_{ij}a_j. \tag{A1}$$

In the equation above, χ^2_{min} is the minimum of χ^2 in the presence of dimension 6 operators, and χ^2_{SM} is the value of χ^2 when all coefficients a_i are zero. The matrix $\mathcal{M}$ is symmetric and positive definite. The first equation makes apparent the values of coefficients a_i that minimize χ^2, which we call $\hat{a}_i$. The second equation is more convenient to use if only a few coefficients a_i are not equal to zero.

a_i	a_{WB}	a_h	a_{ll}^s	a_{ll}^t	a_{lq}^s	a_{lq}^t	a_{le}	a_{qe}	a_{lu}	a_{ld}	a_{ee}
$\hat{a}_i$	$4.1\,10^2$	$-9.3\,10^2$	-5.0	-5.8	$-60.$	-6.9	-0.3	$-23.$	$-4.1\,10^2$	$-7.8\,10^2$	7.5
$\hat{v}_i$	$1.5\,10^2$	$-23.$	$49.$	$76.$	$-1.1\,10^2$	$-2.4\,10^2$	$29.$	$1.4\,10^2$	$-36.$	$-68.$	$44.$

a_i	a_{eu}	a_{ed}	a_{hl}^s	a_{hl}^t	a_{hq}^s	a_{hq}^t	a_{hu}	a_{hd}	a_{he}	a_W
$\hat{a}_i$	$-5.9\,10^2$	$-6.4\,10^2$	$2.3\,10^2$	$19.$	$-77.$	$14.$	$-3.0\,10^2$	$98.$	$4.6\,10^2$	$-4.4\,10^2$
$\hat{v}_i$	$1.0\,10^2$	$15.$	$-6.4\,10^2$	$-88.$	$1.0\,10^2$	$1.7\,10^2$	$71.$	$63.$	$1.8\,10^2$	1.0

TABLE III: Coefficients $\hat{a}_i$ and $\hat{v}_i$ described in Eq. (A1). To obtain values of $\hat{a}_i$ one needs to multiply the numbers in the table times 10^{-8} (GeV)$^{-2}$ and to obtain $\hat{v}_i$ multiply times 10^6 (GeV)^2.

.

The two equivalent sets of coefficients $\hat{a}_i$ and $\hat{v}_i$ are presented in Table III. The elements of matrix $\mathcal{M}$ are listed in Table IV. The dimensions of these elements are easy to read off Eq. (A1) since χ^2 is dimensionless and a_i's have dimension inverse mass squared.

The numerical values of the coefficients $\hat{a}_i$ and $\mathcal{M}_{ij}$ depend on both the experimental values and the SM predictions. Should any of the SM input parameters change in the future, this affects the best fit values $\hat{a}_i$ in Eq. (A1), but not the matrix $\mathcal{M}$. The matrix $\mathcal{M}_{ij}$ only depends on the sizes of errors for different measurements. Thus, $\mathcal{M}$ would change if experimental precision improves in the future. The central, or best fit, values $\hat{a}_i$ depend on all quantities: central values of experiments, the errors, and the SM predictions.

At tree-level, SM predictions depend on well-measured quantities. However the strong coupling constant, the top mass and the Higgs mass all enter at one-loop order. The least known of the three is the Higgs mass and it is interesting to know how the predictions change as the Higgs mass is varied. It is very easy to incorporate changes of the Higgs mass with respect to the assumed reference value of 113 GeV in Ref [19], which we use for the SM predictions. The dominant contribution from the Higgs are corrections to gauge boson propagators and can be incorporated by shifting the S and T parameters [4]. Higgs mass different than its reference value shifts the best fit value $\hat{a}_i$ as follows

$$\delta\hat{a}_{WB} \approx \frac{\alpha}{48\pi scv^2}\log\left(\frac{m_h^2}{m_{h,ref}^2}\right), \quad \delta\hat{a}_h \approx \frac{3\alpha}{8\pi c^2v^2}\log\left(\frac{m_h^2}{m_{h,ref}^2}\right), \tag{A2}$$

where only the leading logarithm in the Higgs mass is kept [4]. This is a good approximation as can be verified by comparing with the exact one-loop result given in Ref. [43].

	a_{WB}	a_h	a_{ll}^s	a_{ll}^t	a_{lq}^s	a_{lq}^t	a_{le}	a_{qe}	a_{lu}	a_{ld}	a_{ee}	a_{eu}	a_{ed}	a_{hl}^s	a_{hl}^t	a_{hq}^s	a_{hq}^t	a_{hu}	a_{hd}	a_{he}	a_W
a_{WB}	9.1e4																				
a_h	2.4e4	7.9e3																			
a_{ll}^s	−78.	−51.	5.8e2																		
a_{ll}^t	−3.9e4	−1.2e4	6.7e2	2.2e4																	
a_{lq}^s	−1.4e3	−1.6e2	0.	1.5e2	2.7e3																
a_{lq}^t	−5.5e2	−1.4e2	0.	5.9e2	4.6e2	2.9e3															
a_{le}	−56.	−9.7	2.8e2	3.0e2	0.	0.	1.3e3														
a_{qe}	1.3e3	72.	0.	−1.4e2	−2.7e2	−7.4e2	0.	2.8e3													
a_{lu}	−4.0e2	3.8	0.	−1.1e2	1.2e3	−2.5e2	0.	−1.2e3	7.1e2												
a_{ld}	−6.9e2	−6.9	0.	66.	1.4e3	3.3e2	0.	−1.4e3	5.8e2	7.8e2											
a_{ee}	−59.	−42.	5.3e2	6.1e2	0.	0.	2.6e2	0.	0.	0.	4.8e2										
a_{eu}	7.8e2	1.1e2	0.	−2.1e2	−1.3e3	−9.1e2	0.	1.4e3	−4.8e2	−7.3e2	0.	8.4e2									
a_{ed}	4.2e2	−83.	0.	1.7e2	−1.3e3	5.5e2	0.	1.3e3	−7.3e2	−6.8e2	0.	4.7e2	8.8e2								
a_{hl}^s	−1.7e4	−4.1e3	1.5e2	9.7e3	−5.9e2	8.3e2	17.	3.7e2	−3.9e2	−1.6e2	1.3e2	66.	3.8e2	5.5e4							
a_{hl}^t	5.9e4	1.7e4	−43.	−3.0e4	−7.1e2	−6.6e2	−31.	6.6e2	−82.	−3.4e2	−32.	4.9e2	47.	1.5e4	6.3e4						
a_{hq}^s	−1.9e3	−1.4e3	0.	2.7e3	−2.6e3	−72.	0.	2.6e3	−1.2e3	−1.4e3	0.	1.2e3	1.4e3	−6.6e3	−8.7e3	6.0e3					
a_{hq}^t	−9.3e3	−4.5e3	0.	8.7e3	−49.	3.5e2	0.	56.	−1.4e2	−36.	0.	−64.	1.8e2	−2.4e4	−3.1e4	7.7e3	2.6e4				
a_{hu}	−6.1e2	−6.6e2	0.	1.2e3	−1.2e3	−4.	0.	1.2e3	−5.1e2	−6.9e2	0.	5.7e2	6.7e2	−3.7e3	−4.4e3	2.2e3	4.1e3	1.4e3			
a_{hd}	1.2e3	4.3e2	0.	−8.1e2	−1.4e3	−1.3e2	0.	1.4e3	−6.9e2	−7.2e2	0.	6.7e2	7.3e2	3.3e3	3.6e3	4.2e2	−2.9e3	1.6e2	1.1e3		
a_{he}	−2.8e4	−4.6e3	−1.1e2	9.0e3	4.6e2	−1.6e2	23.	−4.5e2	2.5e2	2.4e2	−96.	−1.7e2	−3.0e2	−2.5e4	−3.2e4	4.5e3	1.7e4	2.3e3	−2.1e3	3.2e4	
a_W	7.7	4.5	0.	−4.2	0.	0.	0.	0.	0.	0.	0.	0.	0.	6.3	−1.7	0.	0.8	0.	0.	1.4	2.6

TABLE IV: The elements of the matrix $\mathcal{M}$. Since it is a symmetric matrix we do not list the redundant elements. The matrix is equal to the numbers listed above times $10^{12}(\text{GeV})^4$. We abbreviate the powers 10^n as en to save space.
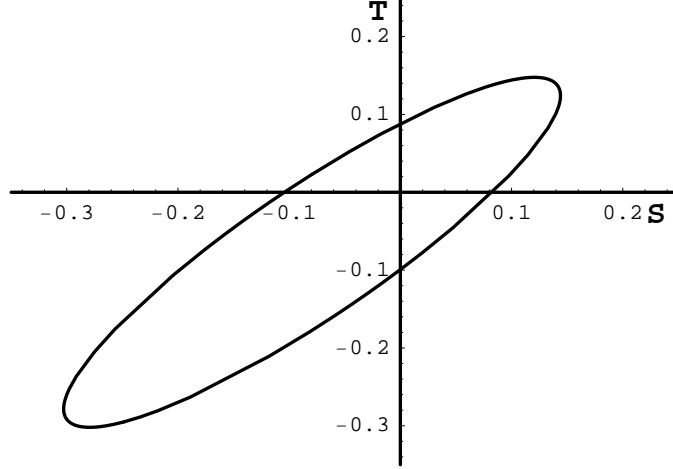
14

FIG. 1: Allowed region for S and T at 90% confidence level obtained using Eq. (B1).

APPENDIX B: S AND T PARAMETERS

In our procedure, the S and T parameters correspond to a_{WB} and a_h as

$$S = \frac{4scv^2 a_{WB}}{\alpha}, \quad T = -\frac{v^2}{2\alpha} a_h.$$

Setting all a_i, but a_{WB} and a_h, to zero in Eq. (A1), we get

$$
\begin{aligned}
\chi^2 &= \chi_0^2 + (a_{WB} \quad a_h) \begin{pmatrix} 9.1\,10^{16} & 2.4\,10^{16} \\ 2.4\,10^{16} & 7.9\,10^{15} \end{pmatrix} \begin{pmatrix} a_{WB} \\ a_h \end{pmatrix} + 1.5\,10^8 a_{WB} - 2.3\,10^7 a_h \\
&= \chi_0^2 + (S \quad T) \begin{pmatrix} 5.4\,10^2 & -4.8\,10^2 \\ -4.8\,10^2 & 5.3\,10^2 \end{pmatrix} \begin{pmatrix} S \\ T \end{pmatrix} + 12.\,S + 5.9\,T.
\end{aligned}
\tag{B1}
$$

A simultaneous fit to S and T using the above equation gives

$$S = -0.08 \pm 0.10, \quad T = -0.08 \pm 0.10.$$

The 1σ error quoted above is obtained by projecting the $\Delta\chi^2 = 1$ ellipse onto the corresponding axis. The plot of the 90% confidence level contour is presented in Fig. 1. Comparing our results with the result in Ref. [19], Figure 10.3, shows good agreement. The results for S and T in Ref. [19] do not include LEP2 measurements, which indicates that LEP2 results do not significantly affect the bounds on the S and T parameters.

APPENDIX C: BOUNDS ON Z' BOSONS

Theoretical and experimental constraints on a color singlet neutral gauge boson are discussed in Ref. [12]. The SM gauge group is extended to include a $U(1)_Z$ factor with Z' its corresponding gauge boson. If the Z' is heavier than the electroweak breaking scale, we can

integrate it out and obtain the following effective Lagrangian:

$$\Delta\mathcal{L} = -\frac{1}{2M_{Z'}^2}g_Z^2 z_H^2 |\phi^\dagger D_\mu \phi|^2 - \sum_{ff'}\frac{1}{4M_{Z'}^2}\frac{1}{1+\delta_{ff'}}g_Z^2 z_f z_{f'}(\bar{f}\gamma^\mu f)(\bar{f'}\gamma_\mu f')$$
$$- \sum_f \left[\frac{i}{4M_{Z'}^2}g_Z^2 z_f z_H(\bar{f}\gamma^\mu \bar{f})(\phi^\dagger D_\mu \phi) + \text{h.c.}\right], \tag{C1}$$

where $M_{Z'}$ is the mass of Z', g_Z is the coupling constant for $U(1)_Z$, and z_H and z_f are the $U(1)_Z$ charges for the Higgs doublet and fermions. These charges satsify [12]

$$z_l = -3z_q, \quad z_e = -3z_q - z_H, \quad z_u = z_H + z_q, \quad z_d = z_q - z_H. \tag{C2}$$

Assuming electromagnetic strength for the Higgs-Z' and fermions-Z' couplings one obtains

$$z_H g_Z = gs, \quad z_q g_Z = \pm gs/3. \tag{C3}$$

The authors of Ref. [12] considered three experimental constraints on $M_{Z'}$: the bound on the T parameter implies a bound $M_{Z'} > 0.9$ TeV; the total decay width of the Z boson, Γ_Z, gives a bound $M_{Z'} > 1.2$ TeV for the $z_q g_Z = -gs/3$ case; and the left-right asymmetry of the electron, A_e, gives a bound $M_{Z'} > 1.0$ TeV for the $z_q g_Z = +gs/3$ case. All the above bounds are given at 95% confidence level.

The T parameter corresponds to the coefficient of the first term in Eq. (C1):

$$T = \frac{v^2}{4\alpha M_{Z'}^2}z_H^2 g_Z^2. \tag{C4}$$

If we use the same value as in Ref. [12], $T = -0.02 \pm 0.13$, we get the same bound for $M_{Z'}$. If we consider individual measurements Γ_Z and A_e, and use the results described in Section IV, we reproduce the other two bounds.

It is interesting to compare these bounds with a global fit to all data. Using our formula Eq. (A1), it takes little effort to obtain a constraint that incorporates simultaneously all operators in the effective Lagrangian (C1). Using Eqs. (C1) and (C2) we obtain all the non-zero coefficients a_i:

$$a_h = -2z_H^2\beta, \quad a_{hf} = -z_H z_f\beta, \quad a_{ff'} = -z_f z_{f'}\beta, \tag{C5}$$

where $\beta = g_Z^2/(4M_{Z'}^2)$. (Cases such as $hf = hq$ are understood to be a_{hq}^s and so on.) Substituting these coefficients in Eq. (A1) and imposing Eq. (C3), we obtain χ^2 as a function of $M_{Z'}$. We then find the bounds for $M_{Z'}$ at 95% confidence level:

$$M_{Z'} > 2.2\text{TeV} \qquad (z_q g_Z = \frac{gs}{3}), \tag{C6}$$

$$M_{Z'} > 2.4\text{TeV} \qquad (z_q g_Z = -\frac{gs}{3}), \tag{C7}$$

which are about twice as large as the bounds given in Ref. [12].

APPENDIX D: A BRIEF INTRODUCTION TO MATHEMATICA PACKAGES.

Numerical calculation of χ^2 was done using Mathematica [44]. Our code can be obtained at *http://pantheon.yale.edu/~zh22/ew.html* or from the authors. We provide two Mathematica no tebooks: *ew_chi2_calculations.nb* and *ew_chi2_results.nb*. The second notebook spares readers from retyping our results by giving the χ^2 distribution in the form in Eq. (A1). It also gives the corresponding errors and the correlation matrix for the coefficients of operators. For those who want to customize our calculation to better suit their purposes, the first notebook contains all the inputs, formulas, and calculations. We briefly describe the structure of the program below. More details are supplied in the comments inside the program.

The notebook *ew_chi2_calculations.nb* is coded in the following order: options, input parameters, measurements, theoretical predictions, and the calculation of χ^2.

Three options have been implemented. First option turns on or off the initial state radiative corrections for fermion pair production at LEP2. (The radiative corrections for $e^+e^- \to e^+e^-$ channel have not been incorporated so far.) Second option toggles if the NuTeV result is included in the calculation of χ^2. The last one controls the presence of second order terms in the coefficients of four-fermion operators at LEP2, see Sec. V.

The input parameters, experimental values, and SM predictions are given next. Should any of these numbers change in the future, one needs to modify the program accordingly.

Next, the deviations from the SM are calculated. All formulas discussed in Sec. IV can be found there. The predictions are presented as the SM values plus corrections proportional to a_i. These predictions are then used to calculate the χ^2 distribution. We have split the total χ^2 to track the contributions from different measurements.

[1] W. Buchmuller and D. Wyler, Nucl. Phys. B **268**, 621 (1986).

[2] B. Grinstein and M. B. Wise, Phys. Lett. B **265**, 326 (1991).

[3] M. Golden and L. Randall, Nucl. Phys. B **361**, 3 (1991); B. Holdom and J. Terning, Phys. Lett. B **247**, 88 (1990); M. E. Peskin and T. Takeuchi, Phys. Rev. Lett. **65**, 964 (1990); G. Altarelli and R. Barbieri, Phys. Lett. B **253**, 161 (1991).

[4] M. E. Peskin and T. Takeuchi, Phys. Rev. D **46**, 381 (1992).

[5] I. Maksymyk, C. P. Burgess and D. London, Phys. Rev. D **50**, 529 (1994) [arXiv:hep-ph/9306267]; C. P. Burgess *et al.* Phys. Lett. B **326**, 276 (1994) [arXiv:hep-ph/9307337].

[6] R. Barbieri, A. Pomarol, R. Rattazzi and A. Strumia, Nucl. Phys. B **703**, 127 (2004) [arXiv:hep-ph/0405040].

[7] A. G. Cohen, H. Georgi and B. Grinstein, Nucl. Phys. B **232**, 61 (1984); H. Georgi, Nucl. Phys. B **363**, 301 (1991).

[8] T. Appelquist and G. H. Wu, Phys. Rev. D **48**, 3235 (1993) [arXiv:hep-ph/9304240].

[9] C. P. Burgess *et al.* Phys. Rev. D **49**, 6115 (1994) [arXiv:hep-ph/9312291].

[10] R. Barbieri and A. Strumia, Phys. Lett. B **462**, 144 (1999) [arXiv:hep-ph/9905281].

[11] C. Arzt, M. B. Einhorn and J. Wudka, Nucl. Phys. B **433**, 41 (1995) [arXiv:hep-ph/9405214].

[12] T. Appelquist, B. A. Dobrescu and A. R. Hopper, Phys. Rev. D **68**, 035012 (2003) [arXiv:hep-ph/0212073].

[13] A. C. Longhitano, Phys. Rev. D **22**, 1166 (1980); Nucl. Phys. B **188**, 118 (1981).

[14] F. Feruglio, Int. J. Mod. Phys. A **8**, 4937 (1993) [arXiv:hep-ph/9301281]; J. Wudka, Int. J. Mod. Phys. A **9**, 2301 (1994) [arXiv:hep-ph/9406205].

[15] H. D. Politzer, Nucl. Phys. B **172**, 349 (1980).

[16] C. Arzt, Phys. Lett. B **342**, 189 (1995) [arXiv:hep-ph/9304230].

[17] B. C. Regan, E. D. Commins, C. J. Schmidt and D. DeMille, Phys. Rev. Lett. **88**, 071805 (2002).

[18] J. Bernabeu, G. A. Gonzalez-Sprinberg and J. Vidal, Nucl. Phys. B **701**, 87 (2004) [arXiv:hep-ph/0404185].

[19] J. Erler and P. Langacker in S. Eidelman *et al.* [Particle Data Group Collaboration], Phys. Lett. B **592**, 1 (2004).

[20] [LEP Collaboration], arXiv:hep-ex/0312023.

[21] C. S. Wood *et al.*, Science **275**, 1759 (1997).

[22] P. A. Vetter *et al.*, Phys. Rev. Lett. **74**, 2658 (1995); N. H.Edwards *et al.*, *ibid* **74**, 2654 (1995).

[23] G. P. Zeller *et al.* [NuTeV Collaboration], Phys. Rev. Lett. **88**, 091802 (2002) [Erratum-ibid. **90**, 239902 (2003)] [arXiv:hep-ex/0110059].

[24] A. Blondel *et al.*, Z. Phys. C **45**, 361 (1990).

[25] J. V. Allaby *et al.* [CHARM Collaboration], Phys. Lett. B **177**, 446 (1986).

[26] K. S. McFarland *et al.* [CCFR Collaboration], Eur. Phys. J. C **1**, 509 (1998) [arXiv:hep-ex/9701010].

[27] P. Vilain *et al.* [CHARM-II Collaboration], Phys. Lett. B **335**, 246 (1994).

[28] G. Abbiendi *et al.* [OPAL Collaboration], Eur. Phys. J. C **33**, 173 (2004) [arXiv:hep-ex/0309053].

[29] P. Achard *et al.* [L3 Collaboration], Phys. Lett. B **600**, 22 (2004) [arXiv:hep-ex/0409016].

[30] V. M. Abazov *et al.* [CDF Collaboration], arXiv:hep-ex/0311039.

[31] G. W. Bennett *et al.* [Muon g-2 Collaboration], Phys. Rev. Lett. **92**, 161802 (2004) [arXiv:hep-ex/0401008].

[32] C. Arzt, M. B. Einhorn and J. Wudka, Phys. Rev. D **49**, 1370 (1994) [arXiv:hep-ph/9304206]; M. B. Einhorn and J. Wudka, Phys. Rev. Lett. **87**, 071805 (2001) [arXiv:hep-ph/0103034].

[33] H. Kroha, Phys. Rev. D **46**, 58 (1992).

[34] K. Hagiwara, R. D. Peccei, D. Zeppenfeld and K. Hikasa, Nucl. Phys. B **282**, 253 (1987).

[35] J. Erler and P. Langacker in K. Hagiwara *et al.* [Particle Data Group Collaboration], Phys. Rev. D **66**, 010001 (2002).

[36] P. Langacker, M. x. Luo and A. K. Mann, Rev. Mod. Phys. **64**, 87 (1992).

[37] D. Y. Bardin *et al.* Comput. Phys. Commun. **133**, 229 (2001) [arXiv:hep-ph/9908433].

[38] A. Denner *et al.* Comput. Phys. Commun. **153**, 462 (2003) [arXiv:hep-ph/0209330].

[39] S. Jadach, W. Placzek and B. F. L. Ward, Phys. Lett. B **390**, 298 (1997) [arXiv:hep-ph/9608412].

[40] P. Abreu *et al.* [DELPHI Collaboration], Eur. Phys. J. C **11**, 383 (1999).

[41] G. Alexander *et al.* [OPAL Collaboration], 130-GeV Phys. Lett. B **387**, 432 (1996).

[42] Pat Ward, private communication.

[43] W. J. Marciano and A. Sirlin, The Phys. Rev. D **22**, 2695 (1980) [Erratum-ibid. D **31**, 213 (1985)].

[44] S. Wolfram, *The Mathematica Book*, Fourth Edition, Cambridge University Press.